

Coherence in Chaos and Caviton Turbulence

G. D. Doolen, D. F. DuBois, and H. A. Rose

Los Alamos National Laboratory, Los Alamos, New Mexico 87545

and

B. Hafizi

Science Applications Inc., Plasma Research Institute, Boulder, Colorado 80302

(Received 8 April 1983)

The chaotic nature of "caviton turbulence" is studied in one-dimensional, many-Fourier-mode numerical simulations of the driven dissipative Zakharov equations. Above the modulational instability threshold the system evolves into a variety of stable patterns of cavitons which become chaotic for stronger driving. The cavitons remain coherent for times long compared to the shortest Lyapunov time.

PACS numbers: 02.50.+s, 03.40.Kf, 52.35.Ra

In this Letter we report on numerical studies in one spatial dimension of a many-mode Fourier representation of the nonlinear partial differential equations known as the Zakharov equations.¹ These equations describe much of the interesting physics of the nonlinear interactions of high-frequency longitudinal electric fields and low-frequency ion-density fluctuations in a nearly collisionless plasma. These studies demonstrate the coexistence of coherent spatial structures—cavitons—and temporal chaos. The level of chaos is measured by the largest positive Lyapunov exponent; the lifetime of the cavitons—density cavities with trapped electrostatic fields—is observed to be long compared to the Lyapunov time. The behavior near the chaotic threshold depends sensitively on the method of driving and on parameters such as the length of the system; at least in the threshold regime the cavitons do not evolve independently.

There have been a number of many-mode numerical simulations of the Zakharov equations² but to our knowledge this is the first quantitative study of the chaotic nature of "caviton turbulence." All of the interesting nonlinear phenomena are observed to occur above the linear threshold for modulational instability of the system driven by the long-wavelength modes. These phenomena include hysteresis effects with stationary solutions (fixed points), limit cycles, two-frequency behavior, and transitions to chaos.³

The Zakharov equations in dimensionless form in Fourier representations are¹

$$i[\partial_t + \nu_e(k) - k^2]E_k(t) = \sum_{k'} n_{k'} E_{k-k'} + S_k(t), \quad (1)$$

$$[\partial_t^2 + 2\nu_i(k)\partial_t + k^2]n_k(t) = -k^2 \sum_{k'} E_{-k'}^*(t)E_{k-k'}(t) \quad (2).$$

supplemented by the complex conjugated Eq. (1) for $E_k^*(t)$. These equations are a useful model of Langmuir turbulence and are discussed elsewhere.¹ Here $E_k(t)$ is the slowly varying envelope of the electrostatic field oscillation at the background plasma frequency and $n_k(t)$ is the Fourier component of the density fluctuation induced by the ponderomotive force which is the right-hand side of Eq. (2). (We have $n_{k=0}=0$.) The dissipation rates $\nu_e(k)$ and $\nu_i(k)$ represent the coupling to the suppressed particle degrees of freedom. We consider only cases in which we are guaranteed the contraction of volumes in solution space.

Equations (1) and (2) were numerically solved by a split-time-step spectral method in which linear terms are advanced in Fourier space and nonlinear terms in real space. Periodic boundary conditions in a box of length L are imposed and from 64 to 1024 Fourier modes were used to ensure adequate resolution of spatial structures. Tests for spatial and temporal resolution were employed, and the dependence on box size was studied.

Numerical experiments were carried out for three methods of driving or energy injection:

(i) Coherent source drive: $S_k(t) = \nu_e W_0^{1/2}$ for $|k| \leq k_{dr}$ ("dr" for "drive") and $S_k = 0$ for $|k| > k_{dr}$.

(ii) Coherent beam drive: $\nu_e(k) = -\nu_{dr}$ for $|k| \leq k_{dr}$ and $\nu_e(k) = \nu_e = \text{constant}$ for $|k| > k_{dr}$.

(iii) Noise source drive: $S_k(t) = \nu_e W_0^{1/2} \xi_k(t)$ for $|k| \leq k_{dr}$ and $S_k = 0$ for $|k| > k_{dr}$, where the $\xi_k(t)$ are delta correlated complex white noise sources of unit rms amplitude.

The measure of chaos in our work will be the Lyapunov exponent which measures the exponential rate of separation of two solutions with nearby initial conditions. Formally the largest Lyapunov

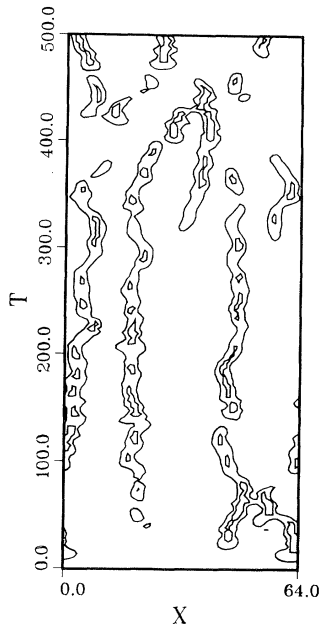


FIG. 1. Contours of equal $|E(x, t)|^2$ vs x and t for the case of a five-mode ($k_{dr} = 0.2$), coherent beam drive [case (ii)], $\nu_{dr} = -0.025$, $\nu_e = 0.05$, $\nu_i = 0.05k$, and $L = 64$, $\bar{W} = 0.13$. The average time spacing between peaks in the caviton "mountain chains" is approximately the Lyapunov time L_1^{-1} .

Lyapunov exponent is given by

$$L_1 = \lim_{t \rightarrow \infty} \lim_{D(0) \rightarrow 0} \{t^{-1} \ln[D(t)/D(0)]\}, \quad (3)$$

where $D(t)$ is the norm of the difference between two solutions: i.e., $D^2(t) = \sum_k D_k^2(t)$, where $D_k^2(t)$, the difference spectrum, is the sum of the squares of the absolute values of these differences in E_k , n_k , and the conjugate variable $u_k = -k^{-2} \bar{n}_k$.

When the variables $E(x, t)$ and $n(x, t)$ evolve from almost flat initial conditions, typically the most modulationally unstable mode ($k \cong W^{1/2}$) evolves into a set of localized structures, the cavitons. Here W is the total electrostatic energy per unit length, $W = \sum_k |E_k(t)|^2 = \int dx |E(x, t)|^2 / L$. In Fig. 1 we show this development for an example of case (ii). An x, t plot of the contours of equal $|E(x, t)|^2$ is given which shows the persistence of the caviton "trajectories" over times long compared to the Lyapunov time. The amplitudes of these cavitons oscillate up and down in time in a random manner; the spacing between peaks is roughly the Lyapunov time, L_1^{-1} .

In Fig. 2 we summarize results for the Lyapunov exponents L_1 vs \bar{W} , where the bar denotes a time average, for various methods of driving and with fixed background dissipation. The caviton lifetime is obtained from contour plots such

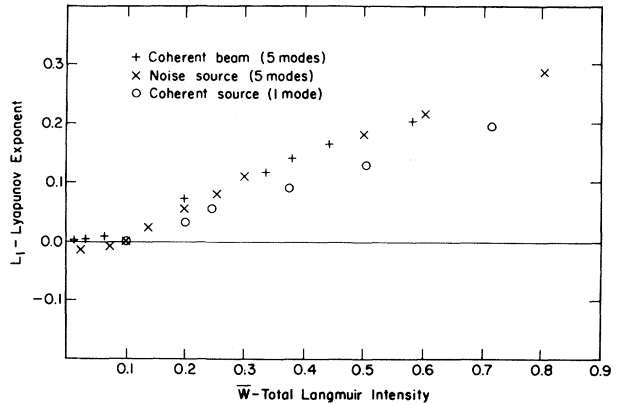


FIG. 2. Lyapunov exponent L_1 vs total energy \bar{W} for several methods of energy injection: crosses, noise driven, and plusses, beam driven, both with five driven modes ($k_{dr} = 0.2$); circles, coherent source drive with one driven mode. In all cases $\nu_e = 0.1$, $\nu_i = 0.1k$.

as Fig. 1 and measurement of the length (in time) of identifiable "caviton mountain chains." A major result of this work is that the cavitons can persist much longer than the Lyapunov time— $\tau_{cav} \times L_1 \gg 1$, indicating the coexistence of spatial coherence and temporal chaos. The largest Lyapunov exponent itself is not a useful measure of the coherence time of the cavitons.

A finite threshold for chaos has been observed for both the coherent-source and noise-source driven cases (see Fig. 2). We have only an incomplete picture of this regime at present; we will here present some results for the case of a single-mode coherent drive [case (i) with $k_{dr} = 0$]. For drive strengths W_0 below the linear modulational instability threshold $W_0(MI) = \nu_e$ for $k = \nu_e^{1/2}$, a trivial fixed point (FP) or stationary solution is observed with $|E_k| = W_0^{1/2} \delta_{k0}$ and $n_k = 0$. Above this threshold we observe complicated hysteresis effects. Among the possible states for $W_0 > W_0(MI)$ is bifurcation to another nontrivial FP with stationary, spatially periodic patterns and characterized by zero momentum, supported by only a few Fourier modes. In this stationary case n is adiabatically related to $|E|^2$; $n = -|E|^2$. For larger W_0 we observe a stable limit cycle (LC); at $W_0 = 0.145$, $W(t)$ oscillates about a mean value of 0.104 with a frequency of 0.50 in our dimensionless units [multiply by $\frac{2}{3}(m_e/m_i)\omega_{pe}$ to obtain physical units]. The contour plots of $|E(x, t)|^2$ and $n(x, t)$ are shown in Figs. 3(a) and 3(b). The overall motion appears as a modulation moving through the cavitons with a speed of $v \cong 0.94$ (times the ion sound speed). The spacing in time between repeated structures in $|E|^2$ agrees with the limit

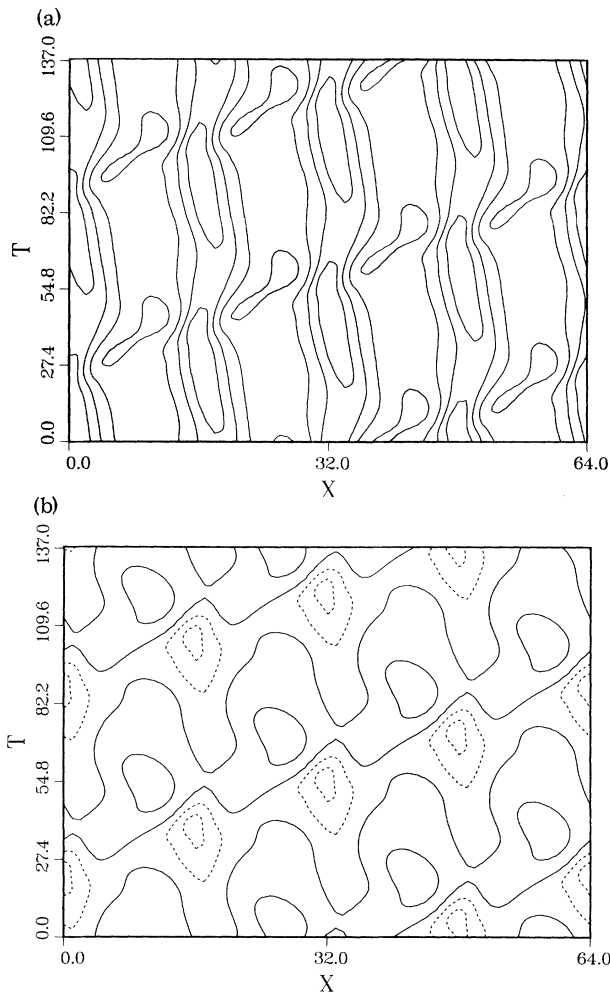


FIG. 3. Behavior above the modulatory threshold $W_0(\text{MI}) = \nu_e = 0.1$ and below chaotic threshold $W_0(\text{chaos}) \sim 0.15$ for a single-mode coherent source drive with $\nu_e = 0.1$, $\nu_i = 0.1k$, and $L = 64$: (a) and (b) contours of $|E(x,t)|^2 = \text{const}$ and $n(x,t) = \text{const}$, respectively, for a stable limit cycle solution at $W_0 = 0.145$. In (a) the lowest values of $|E|^2$ occur in the broad, relatively flat valleys separating caviton "mountain chains." The locations of the cavitons are nearly time independent; their amplitudes oscillate periodically in time but with a timing lag between adjacent cavitons equal to the period of oscillation of $W(t)$. In (b) the dotted contours indicate negative values of n .

cycle period of $W(t)$. We remark that $n(x,t)$ is *not* adiabatically related to $|E(x,t)|^2$ in this case. This stable limit cycle is characterized by a finite momentum and apparently arises from a symmetry-breaking momentum instability.

The stable limit cycle evolves into a two-frequency (TF) state for $W_0 \cong 0.150$. Two frequencies are seen in the time behavior of $W(t)$; the high frequency ω_H is the continuation of the sta-

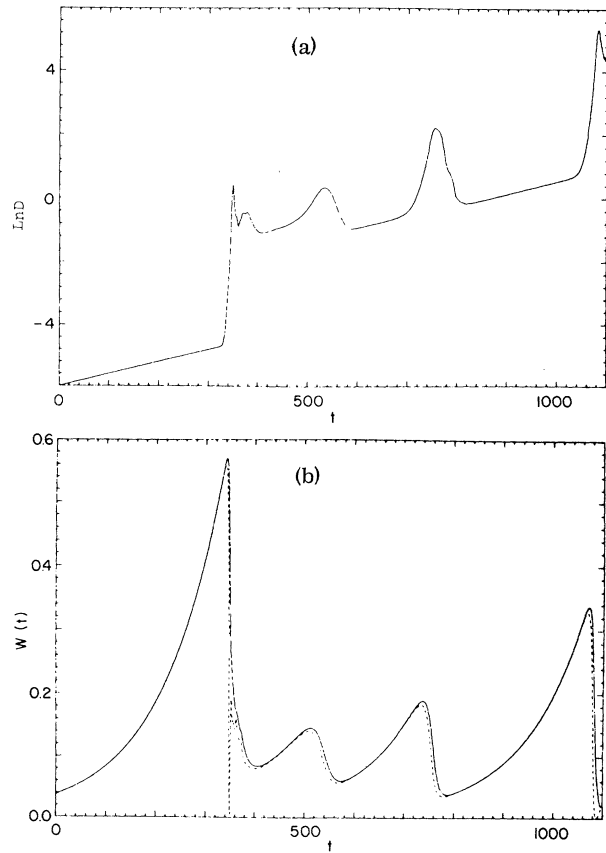


FIG. 4. Illustration of caviton "burst" phenomena: (a) The logarithm of $D(t)$ vs time t for a single-mode coherent beam drive with $\nu_e = 0.1$, $\nu_i = 0.1k$ and $\nu_{dr} = -0.004$, $k_{dr} = 0$, and $L = 64$. (b) For the same case $W(t)$, solid curve, and $W_{k=0}(t) = |E_{k=0}(t)|^2$, dotted curve, vs time t .

ble limit cycle frequency and a new low-frequency modulation ω_L appears with $\omega_H/\omega_L \cong 13$. This case appears to be slightly chaotic. In the corresponding contour plots (not shown here) we observe in this case that the periodicity of the structures observed in Figs. 3(a) and 3(b) is broken. A long-time continuation of this plot reveals that the pattern nearly repeats after about 13 limit cycle periods. We have not yet determined whether these frequencies are commensurate.

We have studied the dependence on system length L of the solutions mentioned above; we observe that the transitions $\text{FP} \leftrightarrow \text{LC}$ and $\text{TF} \leftrightarrow \text{chaos}$ occur for weaker driving in a larger box.

Russell and Ott⁴ have made a study of the threshold regime in a three-mode truncation of the adiabatic limit of the Zakharov equations. We have observed that near the chaotic threshold only a few modes are in fact excited; however, the

many-mode system self-consistently determines which modes are excited.

In Fig. 4(a) $\ln[D(t)]$ and $W_{k=0} \equiv |E_0(t)|^2$ are displayed for a coherent beam drive [case (ii)] where $k_{dr} = 0$. This example illustrates a connection between the traditional concept of the genesis of turbulence by instabilities (in this case the modulational instability), and the more recent concept of stochastic instability. It appears that the local (in time) Lyapunov exponent, $L_1(t) \equiv \dot{D}(t)/D(t)$, can be identified with either the growth rate of the beam unstable mode, or a modulationally unstable mode k_m , for the local value of $W_{k=0}$. The modulational growth rate does not appear in $L_1(t)$ until $W_{k_m} \cong W_{k=0}$. A related analysis of L_1 can be obtained from an average of $D_k(t)$, the difference spectrum,⁵ which shows peaks at $k=0$ and \bar{k}_m . For example, in the interval $0 \leq t \leq 320$, the slope of the curve in Fig. 4(a) is about 0.004, corresponding to the beam unstable mode at $k=0$, while for $320 < t < 350$, $W_{k=0} \cong 0.5$ and the modulational instability growth rate at $k=0.5$ is given by $k[2W_{k=0} - k^2]^{1/2} - \nu_\phi(k) = 0.33$, which is close to the measured slope, 0.30 [an inspection of data not presented here indicates that $E(k=0.5)$ was rapidly growing in this time interval]. It is the nonlinearity of the dynamics which allows for the "turning on and off" of the two types of instabilities, and determines the time-average stochastic instability—the leading Lyapunov exponent. This process also appears to occur for more strongly driven cases in which these instabilities act to produce local bursts of cavitons which occur throughout the system and produce a less intermittent time signature for box averaged quantities.

We have shown that the driven, damped Zakharov equations in one dimension have solutions consisting of regular patterns of cavitons which undergo transitions to temporally chaotic behavior with increasing driving. In the chaotic regime the cavitons have coherence times long compared to the shortest Lyapunov time. A theoretical understanding of these phenomena should have implications for other physical systems which involve the coexistence of coherent structures and chaos.

We are grateful to Professor M. V. Goldman for making available to us an early version of the computer code and for his comments. This research was supported by the U.S. Department of Energy and in part under Contract No. DE-AC03-76-ET53057 with Science Applications, Inc.

¹V. E. Zakharov, Zh. Eksp. Teor. Fiz. **62**, 1745 (1972) [Sov. Phys. JETP **35**, 908 (1972)].

²J. J. Thomson, F. J. Faehl, and W. L. Kruer, Phys. Rev. Lett. **31**, 918 (1973); R. N. Sudan, N. R. Pereira, and J. Denavit, Phys. Fluids **20**, 271 (1977); L. M. Degtyarev, R. Z. Sagdeev, G. I. Solov'ev, V. D. Shapiro, and V. I. Shevchenko, Fiz. Plazmy **6**, 485 (1980) [Sov. J. Plasma Phys. **6**, 283 (1981)]; B. Hafizi, J. C. Weatherall, M. V. Goldman, and D. R. Nicholson, Phys. Fluids **25**, 392 (1982).

³K. Nozaki, Phys. Rev. Lett. **49**, 1883 (1982); A. Bishop, K. Fessler, P. Lomdahl, W. Kerr, M. Williams, and S. Trullinger, Phys. Rev. Lett. **50**, 1095 (1983); K. Nozaki and N. Bekki, Phys. Rev. Lett. **50**, 1226 (1983).

⁴D. A. Russell and E. Ott, Phys. Fluids **24**, 1976 (1981).

⁵R. H. Kraichnan, Phys. Fluids **13**, 569 (1970).